

Models for the Spectral Energy Distributions and Variability of Blazars

M. Böttcher¹

Astrophysical Institute, Department of Physics and Astronomy, Ohio University, Athens, OH, USA

Abstract. In this review, recent progress in theoretical models for blazar emission will be summarized. The salient features of both leptonic and lepto-hadronic approaches to modeling blazar spectral energy distributions will be reviewed. I will present sample modeling results of spectral energy distributions (SEDs) of different types of blazars along the blazar sequence, including *Fermi* high-energy γ -ray data, using both types of models. Special emphasis will be placed on the implications of the recent very-high-energy (VHE) γ -ray detections of non-traditional VHE γ -ray blazars, including intermediate and low-frequency-peaked BL Lac objects and even flat-spectrum radio quasars. Due to the featureless optical spectra of BL Lac objects, the redshifts of several BL Lacs remain unknown. I will briefly discuss possible constraints on their redshift using spectral modeling of their SED including *Fermi* + ground-based VHE γ -ray data. It will be shown that in some cases, spectral modeling with time-independent single-zone models alone is not sufficient to constrain models, as both leptonic and lepto-hadronic models are able to provide acceptable fits to the overall SED. Subsequently, recent developments of time-dependent and inhomogeneous blazar models will be discussed, including detailed numerical simulations as well as a semi-analytical approach to the time-dependent radiation signatures of shock-in-jet models.

1. Introduction

Blazars (BL Lac objects and γ -ray loud flat spectrum radio quasars [FSRQs]) are the most extreme class of active galaxies known. They have been observed at all wavelengths, from radio through VHE γ -rays. The broadband continuum SEDs of blazars are dominated by non-thermal emission and consist of two distinct, broad components: A low-energy component from radio through UV or X-rays, and a high-energy component from X-rays to γ -rays (see, e.g., Figure 1).

Blazars are sub-divided into several types, defined by the location of the peak of the low-energy (synchrotron) SED component. Low-synchrotron-peaked (LSP) blazars, consisting of flat-spectrum radio quasars and low-frequency peaked BL Lac objects (LBLs), have their synchrotron peak in the infrared regime, at $\nu_s \leq 10^{14}$ Hz. Intermediate-synchrotron-peaked (ISP) blazars, consisting of LBLs and intermediate BL Lac objects (IBLs) have their synchrotron peak at optical – UV frequencies at $10^{14} \text{ Hz} < \nu_s \leq 10^{15}$ Hz, while High-synchrotron-peaked (HSP) blazars, almost all known to be high-frequency-peaked BL Lac objects (HBL), have their synchrotron peak at X-ray energies with $\nu_s > 10^{15}$ Hz (Abdo et al. (2010b)). This sequence had first been identified by Fossati et al. (1998), and associated also with a trend of overall decreasing bolometric luminosity as well as decreasing γ -ray dominance along the sequence FSRQ \rightarrow LBL \rightarrow HBL. According to this classification, the bolometric power output of FSRQs is known to be strongly γ -ray dominated, in particular during flaring states, while HBLs are expected to be always synchrotron dominated. However, while the overall

bolometric-luminosity trend still seems to hold, recently, even HBLs seem to undergo episodes of strong γ -ray dominance. A prominent example was the recent joint *Fermi* + HESS observational campaign on the HBL PKS 2155-304 (Aharonian et al. (2009)).

Figure 1 shows examples of blazar SEDs along the blazar sequence, from the FSRQ 3C279 (a), via the LBL BL Lacertae (b) and the IBL 3C 66A (c), to the HBL RGB J0710+591 (d). The sequence of increasing synchrotron peak frequency is clearly visible. However, the *Fermi* spectrum of the LBL BL Lacertae indicates a γ -ray flux clearly below the synchrotron level, while the SED of the IBL 3C 66A is clearly dominated by the *Fermi* γ -ray flux, in contradiction with the traditional blazar sequence.

The emission from blazars is known to be variable at all wavelengths. In particular the high-energy emission from blazars can easily vary by more than an order of magnitude between different observing epochs (von Montigny et al. (1995), Mukherjee et al. (1997), Mukherjee et al. (1999)). However, high-energy variability has been observed on much shorter time scales, in some cases even down to just a few minutes (Aharonian et al. (2007), Albert et al. (2007a)). The flux variability of blazars is often accompanied by spectral changes. Typically, the variability amplitudes are the largest and variability time scales are the shortest at the high-frequency ends of the two SED components. In HBLs, this refers to the X-ray and VHE γ -ray regimes. Such differential spectral variability is sometimes associated with inter-band or intra-band time lags as well as variability patterns which can be characterized as spectral hysteresis in hardness-intensity diagrams (e.g., Takahashi et al. (1996), Kataoka et al. (2000),

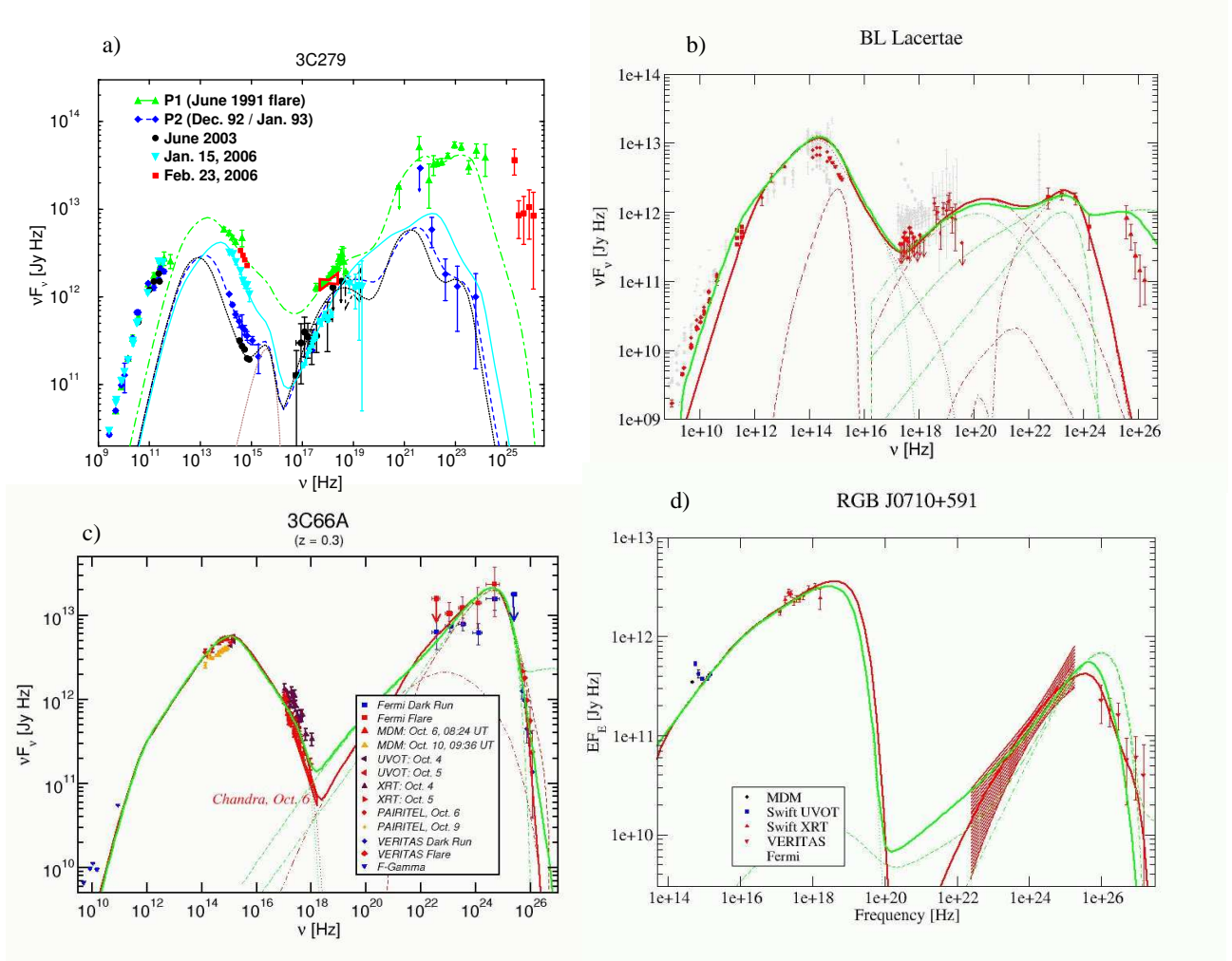


Fig. 1. Spectral energy distributions of four sub-classes of blazars: a) the FSRQ 3C279 (from Collmar et al. (2010)), b) the LBL BL Lacertae, (data from Abdo et al. (2010b)), c) the intermediate BL Lac 3C66A (data from Acciari et al. (2010c)), and d) the HBL RGB J0710+591 (data from Acciari et al. (2010b)). In Panel a) (3C279), lines are one-zone leptonic model fits to SEDs at various epochs shown in the figure. In all other panels, red lines are fits with a leptonic one-zone model; green lines are fits with a one-zone lepto-hadronic model.

Fossati et al. (2000), Zhang et al. (2002)). However, even within the same object this feature tends not to be persistent over multiple observations. Also in other types of blazars, hints of time lags between different observing bands are occasionally found in individual observing campaigns (e.g., Böttcher et al. (2007), Horan et al. (2009)), but the search for time-lag patterns persisting throughout multiple years has so far remained unsuccessful (see, e.g., Hartman et al. (2001) for a systematic search for time lags between optical, X-ray and γ -ray emission in the quasar 3C279).

2. Basic features of leptonic and lepto-hadronic models

The high inferred bolometric luminosities, rapid variability, and apparent superluminal motions provide compelling evidence that the nonthermal continuum emission of blazars is produced in $\lesssim 1$ light day sized emis-

sion regions, propagating relativistically with velocity $\beta\Gamma c$ along a jet directed at a small angle θ_{obs} with respect to our line of sight (for details on the arguments for relativistic Doppler boosting, see Schlickeiser (1996)). Let $\Gamma = (1 - \beta^2)^{-1/2}$ be the bulk Lorentz factor of the emission region, then Doppler boosting is determined by the Doppler factor $D = (\Gamma[1 - \beta \cos \theta_{\text{obs}}])^{-1}$. Let primes denote quantities in the co-moving frame of the emission region, then the observed frequency ν_{obs} is related to the emitted frequency through $\nu_{\text{obs}} = D\nu'/(1+z)$, where z is the redshift of the source, and the energy fluxes are connected through $F_{\nu_{\text{obs}}}^{\text{obs}} = D^3 F_{\nu'}'$. Intrinsic variability on a co-moving time scale t'_{var} will be observed on a time scale $t_{\text{var}}^{\text{obs}} = t'_{\text{var}}(1+z)/D$. Using the latter transformation along with causality arguments, any observed variability leads to an upper limit on the size scale of the emission region through $R \lesssim ct_{\text{var}}^{\text{obs}} D/(1+z)$.

While the electron-synchrotron origin of the low-frequency emission is well established, there are two funda-

mentally different approaches concerning the high-energy emission. If protons are not accelerated to sufficiently high energies to reach the threshold for $p\gamma$ pion production on synchrotron and/or external photons and to contribute significantly to high-energy emission through proton-synchrotron radiation, the high-energy radiation will be dominated by emission from ultrarelativistic electrons and/or pairs (leptonic models). In the opposite case, the high-energy emission will be dominated by cascades initiated by $p\gamma$ pair and pion production as well as proton, π^\pm , and μ^\pm synchrotron radiation, while primary leptons are still responsible for the low-frequency synchrotron emission (lepto-hadronic models). The following sub-sections provide a brief overview of the main radiation physics aspects of both leptonic and lepto-hadronic models.

2.1. Leptonic models

In leptonic models, the high-energy emission is produced via Compton upscattering of soft photons off the same ultrarelativistic electrons which are producing the synchrotron emission. Both the synchrotron photons produced within the jet (the SSC process: Marscher & Gear (1985), Maraschi et al. (1992), Bloom & Marscher (1996)), and external photons (the EC process) can serve as target photons for Compton scattering. Possible sources of external seed photons include the accretion disk radiation (e.g., Dermer et al. (1992), Dermer & Schlickeiser (1993)), reprocessed optical – UV emission from circumnuclear material (e.g., the BLR; Sikora et al. (1994), Blandford & Levinson (1995), Ghisellini & Madau (1996), Dermer et al. (1997)), infrared emission from a dust torus (Blażejowski et al. (2000)), or synchrotron emission from other (faster/slower) regions of the jet itself (Georganopoulos & Kazanas (2003), Ghisellini & Tavecchio (2008)).

The relativistic Doppler boosting discussed above allows one to choose model parameters in a way that the $\gamma\gamma$ absorption opacity of the emission region is low throughout most of the high-energy spectrum (i.e., low compactness). However, at the highest photon energies, this effect may make a non-negligible contribution to the formation of the emerging spectrum (Aharonian et al. (2008)) and re-process some of the radiated power to lower frequencies. Also the deceleration of the jets may have a significant impact on the observable properties of blazar emission through the radiative interaction of emission regions with different speed (Georganopoulos & Kazanas (2003), Ghisellini et al. (2005)) and a varying Doppler factor (Böttcher & Principe (2009)). Varying Doppler factors may also be a result of a slight change in the jet orientation without a substantial change in speed, e.g., in a helical-jet configuration (e.g., Villata & Raiteri (1999)). In the case of ordered magnetic-field structures in the emission region, such a helical configuration should have observable

synchrotron polarization signatures, such as the prominent polarization-angle swing recently observed in conjunction with an optical + *Fermi* γ -ray flare of 3C 279 (Abdo et al. (2010a)).

In the most simplistic approaches, the underlying lepton (electrons and/or positrons) distribution is ad-hoc pre-specified, either as a single or broken power-law with a low- and high-energy cut-off. While leptonic models under this assumption have been successful in modeling blazar SEDs (e.g., Ghisellini et al. (1998)), they lack a self-consistent basis for the shape of the electron distribution. A more realistic approach consists of the self-consistent steady-state solution of the Fokker-Planck equation including a physically motivated (e.g., from shock-acceleration theory) acceleration of particles and all relevant radiative and adiabatic cooling mechanisms (e.g., Ghisellini & Tavecchio (2009), Acciari et al. (2009b), Weidinger et al. (2010)). The model described in Acciari et al. (2009b), based on the time-dependent model of Böttcher & Chiang (2002), has been used to produce the leptonic model fits shown in Fig. 1.

In order to reproduce not only broadband SEDs, but also variability patterns, the time-dependent electron dynamics and radiation transfer problem has to be solved self-consistently. Such time-dependent SSC models have been developed by, e.g., Mastichiadis & Kirk (1997), Kataoka et al. (2000), Li & Kusunose (2000), Sokolov et al. (2004). External radiation fields have been included in such treatments in, e.g., Sikora et al. (2001), Böttcher & Chiang (2002), Sokolov & Marscher (2005).

Leptonic models have generally been very successfully applied to model the SEDs and spectral variability of blazars. The radiative cooling time scales (in the observers's frame) of synchrotron-emitting electrons in a typical $B \sim 1$ G magnetic field are of order of several hours – ~ 1 d at optical frequencies and $\lesssim 1$ hr in X-rays and hence compatible with the observed intra-day variability. However, the recent observation of extremely rapid VHE γ -ray variability on time scales of a few minutes poses severe problems to simple one-zone leptonic emission models. Even with large bulk Lorentz factors of ~ 50 , causality requires a size of the emitting region that might be smaller than the Schwarzschild radius of the central black hole of the AGN (Begelman et al. (2008)). As a possible solution, it has been suggested (Tavecchio & Ghisellini (2008)) that the γ -ray emission region may, in fact, be only a small spine of ultrarelativistic plasma within a larger, slower-moving jet. Such fast-moving small-scale jets could plausibly be powered by magnetic reconnection in a Poynting-flux dominated jet, as proposed by Giannios et al. (2009).

2.2. Lepto-hadronic models

If a significant fraction of the jet power is converted into the acceleration of relativistic pro-

tons in a strongly magnetized environment, reaching the threshold for $p\gamma$ pion production, synchrotron-supported pair cascades will develop (Mannheim & Biermann (1992), Mannheim (1993)). The acceleration of protons to the necessary ultra-relativistic energies ($E_p^{\max} \gtrsim 10^{19}$ eV) requires high magnetic fields of several tens of Gauss to constrain the Larmor radius $R_L = 3.3 \times 10^{15} B_1^{-1} E_{19}$ cm, where $B = 10 B_1$ G, and $E_p = 10^{19} E_{19}$ eV, to be smaller than the size of the emission region, typically inferred to be $R \lesssim 10^{16}$ cm from the observed variability time scale. In the presence of such high magnetic fields, the synchrotron radiation of the primary protons (Aharonian (2000), Mücke & Protheroe (2000)) and of secondary muons and mesons (Rachen & Mészáros (1998), Mücke & Protheroe (2000), Mücke & Protheroe (2001), Mücke et al. (2003)) must be taken into account in order to construct a self-consistent synchrotron-proton blazar (SPB) model. Electromagnetic cascades can be initiated by photons from π^0 -decay (“ π^0 cascade”), electrons from the $\pi^\pm \rightarrow \mu^\pm \rightarrow e^\pm$ decay (“ π^\pm cascade”), p -synchrotron photons (“ p -synchrotron cascade”), and μ^- , π^- and K -synchrotron photons (“ μ^\pm -synchrotron cascade”).

Mücke & Protheroe (2001) and Mücke et al. (2003) have shown that the “ π^0 cascades” and “ π^\pm cascades” from ultra-high energy protons generate featureless γ -ray spectra, in contrast to “ p -synchrotron cascades” and “ μ^\pm -synchrotron cascades” that produce a two-component γ -ray spectrum. In general, direct proton and μ^\pm synchrotron radiation is mainly responsible for the high energy bump in blazars, whereas the low energy bump is dominated by synchrotron radiation from the primary e^- , with a contribution from secondary electrons.

Hadronic blazar models have so far been very difficult to investigate in a time-dependent way because of the very time-consuming nature of the required Monte-Carlo cascade simulations. In general, it appears that it is difficult to reconcile very rapid high-energy variability with the radiative cooling time scales of protons, e.g., due to synchrotron emission, which is $t_{\text{sy}}^{\text{obs}} = 4.5 \times 10^5 (1+z) D_1^{-1} B_1^{-2} E_{19}^{-1}$ s (Aharonian (2000)), i.e., of the order of several days for ~ 10 G magnetic fields and typical Doppler factors $D = 10 D_1$. However, rapid variability on time scales shorter than the proton cooling time scale may be caused by geometrical effects.

In order to avoid time-consuming Monte-Carlo simulations of the hadronic processes and cascades involved in lepto-hadronic models, one may consider a simplified prescription of the hadronic processes. Kelner & Aharonian (2008) have produced analytic fit functions to Monte-Carlo generated results of hadronic interactions using the SOFIA code (Mücke et al. (2000)). Those fits describe the spectra of the final decay products, such as electrons, positrons, neutrinos, and photons from π^0 decay. The use of those functions requires a prior knowledge of the target photon field (in the SPB model

the electron-synchrotron photon field) as well as the proton spectrum. Once the first-generation products are evaluated, one still needs to take into account the effect of cascading, as the synchrotron emission from most of the electrons (and positrons) as well as π^0 decay γ -rays are produced at \gg TeV energies, where the emission region is highly opaque to $\gamma\gamma$ pair production. A quasi-analytical description of the cascades can be found as follows.

We start with the injection rates of first-generation high-energy γ -rays, \dot{N}_e^0 , and pairs, $Q_e(\gamma)$, from the analytical fit functions of Kelner & Aharonian (2008). The cascades are usually well described as linear cascades so that the optical depth for $\gamma\gamma$ absorption, $\tau_{\gamma\gamma}(\epsilon)$ can be pre-calculated from the low-energy radiation field. Under these conditions, the spectrum of escaping (observable) photons can be calculated as

$$\dot{N}_e^{\text{esc}} = \dot{N}_e^{\text{em}} \left(\frac{1 - e^{-\tau_{\gamma\gamma}[\epsilon]}}{\tau_{\gamma\gamma}[\epsilon]} \right) \quad (1)$$

where \dot{N}_e^{em} has contributions from the first-generation high-energy photon spectrum and synchrotron emission from secondaries, $\dot{N}_e^{\text{em}} = \dot{N}_e^0 + \dot{N}_e^{\text{sy}}$. A fairly accurate evaluation of the synchrotron spectrum is achieved with a single-electron emissivity of the form $j_\nu \propto \nu^{1/3} e^{-\epsilon/\epsilon_0}$ with $\epsilon_0 = b \gamma^2$, where $b \equiv B/B_{\text{crit}}$ and $B_{\text{crit}} = 4.4 \times 10^{13}$ G. The electron distribution, $N_e(\gamma)$ will be the solution to the isotropic Fokker-Planck equation in equilibrium ($\partial \langle \cdot \rangle / \partial t = 0$):

$$\frac{\partial}{\partial \gamma} (\dot{\gamma} N_e[\gamma]) = Q_e(\gamma) + \dot{N}_e^{\gamma\gamma}(\gamma) + \dot{N}_e(\gamma)^{\text{esc}}. \quad (2)$$

For the high magnetic fields of $B \gtrsim 10$ G, as required for hadronically dominated γ -ray emission, electron cooling will be dominated by synchrotron losses, i.e., $\dot{\gamma} = -\nu_0 \gamma^2$ with $\nu_0 = (4/3) c \sigma_T u_B / (m_e c^2)$. We are only interested in high-energy particles emitting synchrotron radiation at least at X-ray energies. For those particles, the synchrotron cooling time scale is expected to be much shorter than the escape time scale so that the escape term in Eq. 2 may be neglected. $\dot{N}_e^{\gamma\gamma}(\gamma)$ in Eq. 2 is the rate of particle injection due to $\gamma\gamma$ absorption, to be evaluated self-consistently with the radiation field. In the $\gamma\gamma$ absorption of a high-energy photon of energy ϵ , one of the produced particles will assume the major fraction, f_γ of the photon energy. Hence, an electron/positron pair with energies $\gamma_1 = f_\gamma \epsilon$ and $\gamma_2 = (1 - f_\gamma) \epsilon$ is produced. Furthermore realizing that every non-escaping photon (according to Eq.1) will produce an electron/positron pair, we can write the pair production rate as

$$\dot{N}_e^{\gamma\gamma}(\gamma) = f_{\text{abs}}(\epsilon_1) \left(\dot{N}_{\epsilon_1}^0 + \dot{N}_{\epsilon_1}^{\text{sy}} \right) + f_{\text{abs}}(\epsilon_2) \left(\dot{N}_{\epsilon_2}^0 + \dot{N}_{\epsilon_2}^{\text{sy}} \right) \quad (3)$$

where $\epsilon_1 = \gamma/f_\gamma$, $\epsilon_2 = \gamma/(1 - f_\gamma)$ and $f_{\text{abs}}(\epsilon) \equiv 1 - (1 - e^{-\tau_{\gamma\gamma}[\epsilon]})/\tau_{\gamma\gamma}[\epsilon]$. With this approximation, we find an implicit solution to Equation 2:

$$N_e(\gamma) = \frac{1}{\nu_0 \gamma^2} \int_\gamma^\infty d\tilde{\gamma} \left\{ Q_e(\tilde{\gamma}) + \dot{N}_e^{\gamma\gamma}(\tilde{\gamma}) \right\} \quad (4)$$

The solution (4) is implicit in the sense that the particle spectrum $N_e(\gamma)$ occurs on both sides of the equation as $\dot{N}_e^{\gamma\gamma}$ depends on the synchrotron emissivity, which requires knowledge of $N_e(\tilde{\gamma})$, where pairs at energies of $\tilde{\gamma}_1 = \sqrt{\gamma/(f_\gamma b)}$ and $\tilde{\gamma}_2 = \sqrt{\gamma/([1 - f_\gamma] b)}$ provide the majority of the radiative output relevant for pair production at energy γ . However, for practical applications, one may use the fact that generally, γ , the argument on the l.h.s., is much smaller than $\tilde{\gamma}_{1,2}$. This condition is fulfilled if there is no pion-induced pair injection at energies above $\gamma_{\text{crit}} = 4.4 \times 10^{13} ([1 - f_\gamma] B_G)^{-1}$ or $E_{e,\text{crit}} = 2.3 \times 10^{19} ([1 - f_\gamma] B_G)^{-1}$ eV. In a usual synchrotron-proton-blazar model setup, no substantial pair injection above $E_{e,\text{crit}}$ is expected. Therefore, Eq. 4 may be evaluated progressively, starting at the highest pair energies for which $Q_0(\gamma) \neq 0$ or $\dot{N}_{e,1,2}^0 \neq 0$, and then using the solution for $N_e(\gamma)$ for large γ as one progresses towards lower values of γ .

Once the equilibrium pair distribution $N_e(\gamma)$ is known, it can be used to evaluate the synchrotron emissivity and hence, using Eq. 1 the observable photon spectrum.

Example model fits to several blazar SEDs using a simplified lepto-hadronic model based on the Kelner & Aharonian (2008) fit functions and the above cascade description are shown in Fig 1, b) – d) and compared to leptonic models of the same SEDs. As the low-frequency component is electron-synchrotron emission from primary electrons, it is not surprising that virtually identical fits to the synchrotron component can be provided in both types of models. In the high-frequency component, strongly peaked spectral shapes, as, e.g., in 3C 66A and RGB J0710+591 require a strong proton-synchrotron dominance with the cascading of higher-energy (\gg TeV) emission only making a minor contribution to the high-energy emission. This, in fact, makes it difficult to achieve a substantial extension of the escaping high-energy emission into the > 100 GeV VHE γ -ray regime. In objects with a smoother high-energy SED, e.g., BL Lacertae in Fig. 1b, a substantially larger contribution from cascade emission (and leptonic SSC emission) is allowed to account for a relatively high level of hard X-ray / soft γ -ray emission. This also allows for a substantial extension of the γ -ray spectrum into the VHE regime.

3. Spectral fits along the blazar sequence

In the framework of leptonic models, the blazar sequence FSRQ \rightarrow LBL \rightarrow IBL \rightarrow HBL is often modeled through a decreasing contribution of external radiation fields to radiative cooling of electrons and production of high-energy emission (Ghisellini et al. (1998)). In this sense, HBLs have traditionally been well represented by pure synchrotron-self-Compton models, while FSRQs often require a substantial EC component. This interpretation is consistent with the observed strong emission lines in FSRQs, which are absent in BL Lac objects. At the same time, the denser circumnuclear environment in quasars might also lead to a higher accretion rate and hence a more

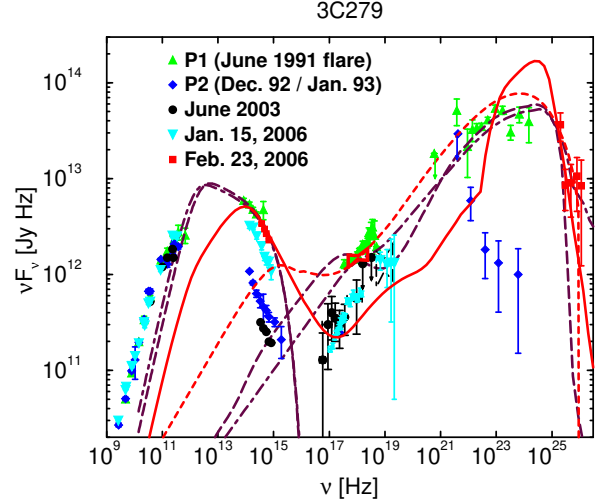


Fig. 2. Fits to the SED of 3C279 during the time of the MAGIC detection (Albert et al. (2008)). The heavy solid curve is an attempt of a leptonic model with EC-dominated γ -ray emission, while the dotted curve is an SSC fit to the X-ray through γ -ray spectrum. The dashed and dot-dashed curves are hadronic model fits.

powerful jet, consistent with the overall trend of bolometric luminosities along the blazar sequence. This may even be related to an evolutionary sequence from FSRQs to HBLs governed by the gradual depletion of the circumnuclear environment (Böttcher & Dermer (2002)).

However, in this interpretation, it would be expected that mostly HBLs (and maybe IBLs) should be detectable as emitters of VHE γ -rays since in LBLs and FSRQs, electrons are not expected to reach \sim TeV energies. This appears to contradict the recent VHE γ -ray detections of lower-frequency peaked objects such as W Comae (Acciari et al. (2008)), 3C66A (Acciari et al. (2009a)), PKS 1424+240 (Acciari et al. (2010a)), BL Lacertae (Albert et al. (2007b)), S5 0716+714 (Anderhub et al. (209)), and even the FSRQs 3C 279 (Albert et al. (2008)) and PKS 1510-089 (Wagner & Behera (2010)).

The overall SEDs of IBLs detected by VERITAS could still be fit satisfactorily with a purely leptonic model. Fitting the SEDs of the IBLs 3C66A and W Comae with a pure SSC model, while formally possible, would require rather extreme parameters. In particular, magnetic fields several orders of magnitude below equipartition would be needed, which might pose a severe problem for jet collimation. Much more natural fit parameters can be adopted when including an EC component with an infrared radiation field as target photons (Acciari et al. (2009b), Acciari et al. (2010c)).

In Böttcher et al. (2009) it has been demonstrated that the VHE γ -ray detection of the FSRQ 3C 279 poses severe problems for any variation of single-zone leptonic jet model. The SED with the MAGIC points is shown in Fig. 2, along with attempted leptonic as well as hadronic

model fits. The fundamental problem for the leptonic model interpretation is the extremely wide separation between the synchrotron and γ -ray peak frequencies. In a single-zone SSC interpretation this would require a very high Lorentz factor of electrons at the peak of the electron distribution and, in turn, an extremely low magnetic field. In an EC interpretation (the solid curve in Fig. 2) the SSC component, usually dominating the X-ray emission in leptonic fits to FSRQs like 3C 279, is too far suppressed to model the simultaneous RXTE spectrum. As an alternative, the optical emission could be produced in a separate emission component. A pure SSC fit to the X-ray and γ -ray component (the short-dashed curve in Fig. 2) is technically possible, but also requires a far sub-equipartition magnetic field. Much more natural parameters could be achieved in a fit with the synchrotron-proton-blazar model (Mücke et al. (2003)), as illustrated by the long-dashed and dot-dashed model curves in Fig. 2.

4. Redshift constraints from blazar SED modeling

BL Lac objects are defined by the absence of broad emission lines in their optical spectra. This makes the determination of their redshifts, and hence distances, very difficult, and in many cases even impossible. Photometric redshifts, estimated under the assumption that the host galaxies of BL Lac objects are nearly standard candles (e.g., Sbarufatti et al. (2005)), are still highly uncertain, and optical spectroscopy often yields only lower limits on redshifts (e.g., Finke et al. (2007)).

An alternative method of estimating BL Lac redshifts exploits the fact that high-energy and VHE γ -rays are absorbed through $\gamma\gamma$ pair production on the Extragalactic Background Light (EBL), see, e.g., Dwek & Krennrich (2005), Stecker et al. (2006), Franceschini et al. (2008), Gilmore et al. (2009), Finke et al. (2010). Substantial progress has been made in the last few years so that the accepted models of the EBL spectrum are now converging to an EBL level near the lower limit set by direct galaxy counts (e.g., Aharonian et al. (2006), Abdo et al. (2010c)).

Exploiting this improved knowledge of the EBL spectrum and intensity, limits on VHE γ -ray blazars can now be set from the expectation that the intrinsic (unabsorbed by the EBL) HE to VHE γ -ray spectra of blazars are not becoming harder towards higher energies. A robust upper limit to the source redshift can therefore be found by considering a straight power-law extrapolation of the best-fit *Fermi* power-law spectrum into the VHE γ -ray regime, and attributing the change in spectral slope towards the measured VHE spectrum purely to EBL absorption (e.g., Georganopoulos et al. (2010), Acciari et al. (2010a)). A somewhat more realistic approach has been suggested by Prandini et al. (2010), taking into account the expected intrinsic softening of the VHE γ -ray spectrum, based on a sample of blazars with known redshifts detected both by *Fermi* and ground-based VHE γ -ray observatories.

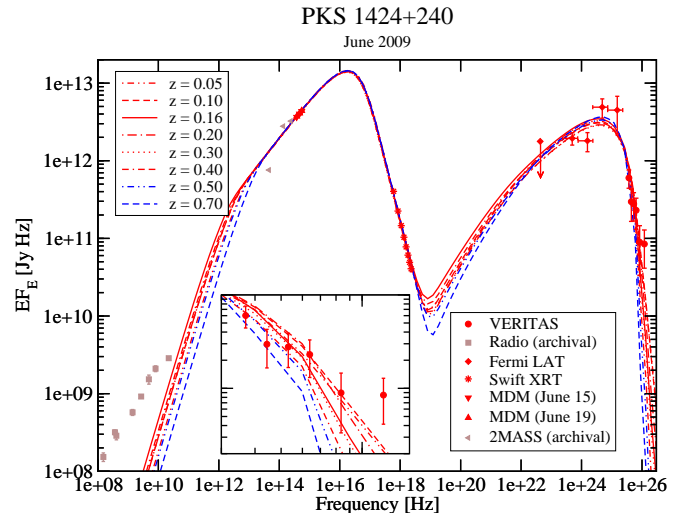


Fig. 3. Fits to the SED of PKS 1424+240, assuming a range of plausible redshifts (from Acciari et al. (2010a)). All SEDs have been corrected for $\gamma\gamma$ absorption by the EBL using the model of Gilmore et al. (2009). The inset shows a zoom-in on the VHE γ -ray spectrum. The spectral fits favour a source redshift of $z < 0.4$.

If the SED of a blazar with unknown redshift is well sampled, the EBL absorption effect can be exploited in an even more sophisticated way by constraining models through the SED from the optical to GeV γ -rays and varying the redshift to yield the best fit to the measured VHE γ -ray spectrum. This procedure has been carried out in detail for the recent VERITAS detections of PKS 1424+240 (Acciari et al. (2010a)) and 3C66A (Acciari et al. (2010c)).

In the case of PKS 1424+240, only very unreliable redshift estimates were available. Fig. 3 shows our suite of models for a wide range of plausible redshifts. While a straight power-law extrapolation of the *Fermi* spectrum yields an upper limit of $z < 0.6$, our spectral model (leptonic SSC) clearly favors a redshift of $z < 0.4$. The redshift of 3C 66A is usually quoted as $z = 0.444$, but is actually highly uncertain as well (Bramel et al. (2005)). A scan through redshifts yielded a preferred redshift of $z \sim 0.2 - 0.3$ for this object, in good agreement with the estimate found by Prandini et al. (2010). The leptonic model fit to 3C66A shown in Fig. 1c is based on a redshift of $z = 0.3$.

5. Inhomogeneous jet models

The complicated and often inconsistent variability features found in blazars provide a strong motivation to investigate jet models beyond a simple, spherical, one-zone geometry. The idea behind phenomenological multi-zone models like the spine-sheath model of Tavecchio & Ghisellini (2008) or the decelerating-jet model of Georganopoulos & Kazanas (2003) was that differential relativistic motion between various emission zones will lead to Doppler boosting of one zone's emis-

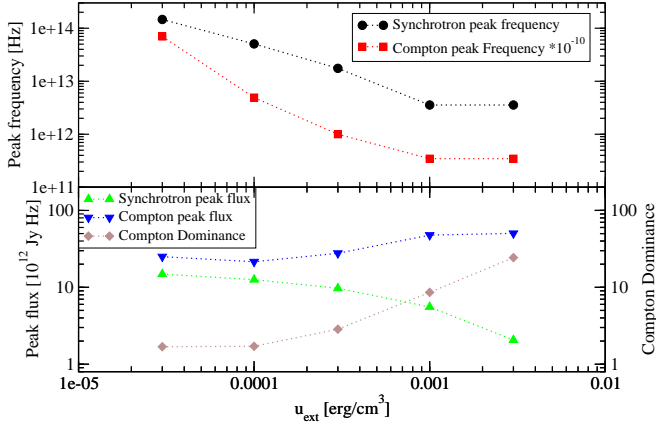


Fig. 4. Dependence of the SED characteristics of time-averaged spectra from the internal-shock model, on the external radiation energy density u_{ext} .

sion into the rest frame of another zone. This can reduce the requirements of extreme bulk Lorentz (and Doppler) factors inferred from simple one-zone leptonic modeling of rapidly variable VHE γ -ray blazars, such as Mrk 501 or PKS 2155-304, and has led to successful model fits to the SEDs of those sources with much more reasonable model parameters.

However, the models mentioned above do not treat the radiation transport and electron dynamics in a time-dependent way and do therefore not make any robust predictions concerning variability and inter-band cross-correlations and time lags. In order to address those issues, much work has recently been devoted to the investigation of the radiative and timing signatures of shock-in-jet models, which will be summarized in the following sub-section.

5.1. Shock-in-jet models

Early versions of shock-in-jet models were developed with focus on explaining radio spectra of extragalactic jets, e.g., by Marscher & Gear (1985). Their application to high-energy spectra of blazars was proposed by Spada et al. (2001). Detailed treatments of the electron energization and dynamics and the radiation transfer in a standing shock (Mach disk) in a blazar jet were developed by Sokolov et al. (2004), Sokolov & Marscher (2005), Graff et al. (2008). The internal-shock model discussed in Mimica et al. (2004), Joshi (2009) assumes that the central engine is intermittently ejecting shells of relativistic plasma at varying speeds, which subsequently collide. Such models have had remarkable success in explaining SEDs and time lag features of generic blazars.

The realistic treatment of radiation transfer in an internal-shock model for a blazar requires the time-dependent evaluation of retarded radiation fields originating from all parts of the shocked regions of the jet. The model system is therefore highly non-linear and can generally only be solved using numerical simulations (e.g., Sokolov et al. (2004), Mimica et al. (2004),

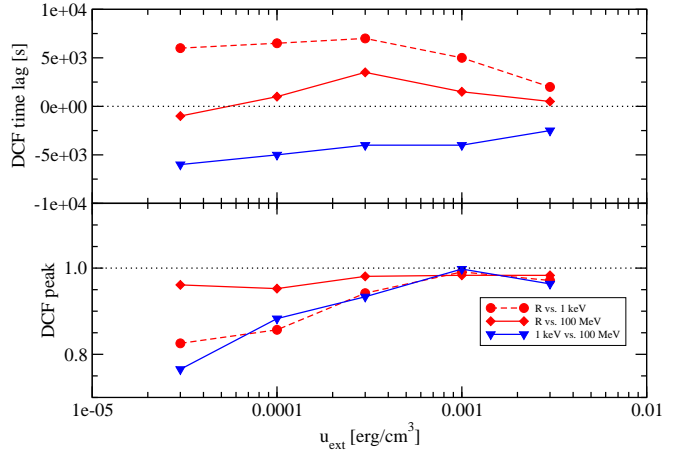


Fig. 5. Dependence on inter-band cross correlations and time lags on the external radiation energy density.

Graff et al. (2008)). As the current detailed internal-shock models employ either full expressions or accurate approximations to the full emissivities of synchrotron and Compton emission, a complete simulation of the time-dependent spectra and light curves is time-consuming and does therefore generally not allow to efficiently explore a large parameter space. General patterns of the SED, light curves and expected time lags between different wavelength bands have been demonstrated for very specific, but observationally very poorly constrained, sets of parameters.

To remedy this aspect, Böttcher & Dermer (2010) have developed a semi-analytical internal-shock model for blazars. In this model, the time- and space-dependent electron spectra, affected by shock acceleration behind the forward and reverse shocks, and subsequent radiative cooling, is calculated fully analytically. Taking into account all light travel time effects, the observed synchrotron and external-Compton spectra are also evaluated fully analytically, using a δ -function approximation to the emissivities. The evaluation of the SSC emission still requires a two-dimensional numerical integration.

This semi-analytical model allowed the authors to efficiently scan a substantial region of parameter space and discuss the dependence on the characteristics of time-averaged SEDs, as well as cross-band correlations and time lags. As an example, Fig. 4 shows the dependence of the SED characteristics on the external radiation field energy density, u_{ext} . In the classical interpretation of the blazar sequence, an increasing u_{ext} corresponds to a transition from BL Lac spectral characteristics to FSRQ-like characteristics. The decreasing synchrotron peak frequency and increasing Compton dominance found in the parameter study are reproducing this effect.

From the internal-shock simulations, energy-dependent light curves could be extracted. Using the standard Discrete Correlation Function (DCF: Edelson & Krolik (1988)) analysis, inter-band time lags could be extracted for any set of parameters. Fig. 5 shows

the dependence of the inter-band time lags between optical, X-ray and *Fermi* γ -ray light curves (top panel) and the quality of the cross correlation, characterized by the peak value of the DCF (bottom panel) as a function of the external radiation energy density.

One of the most remarkable results of this study was that only slight changes in physical parameters can lead to substantial changes of the inter-band time lags and even a reversal of the sign of the lags. This may explain the lack of consistency of lags even within the same source.

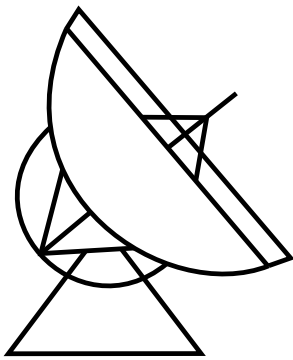
Acknowledgements. I thank Manasvita Joshi for careful proofreading of the manuscript and helpful comments. I acknowledge support from NASA through Fermi Guest Investigator Grants NNX09AT81G and NNX09AT82G, XMM-Newton Guest Investigator grant NNX09AV45G, as well as Astrophysics Theory Program grant NNX10AC79G.

References

- Abdo, A. A., et al., 2010, *Nature*, 463, 919
 Abdo, A. A., et al., 2010b, *ApJ*, 716, 30
 Abdo, A. A., et al., 2010c, *ApJ*, submitted (arXiv:1005.0996)
 Acciari, V. A., 2008, *ApJ*, 684, L73
 Acciari, V. A., 2009a, *ApJ*, 693, L104
 Acciari, V. A., 2009b, *ApJ*, 707, 612
 Acciari, V. A., et al., 2010a, *ApJ*, 708, L100
 Acciari, V. A., et al., 2010b, *ApJ*, 715, L49
 Acciari, V. A., et al., 2010c, in preparation
 Aharonian, F. A., 2000, *New Astron.*, 5, 377
 Aharonian, F. A., 2006, *Nature*, 440, 1018
 Aharonian, F. A., et al., 2007, *ApJ*, 664, L71
 Aharonian, F. A., Khargulyan, D., & Costamante, L., 2008, *MNRAS*, 387, 1206
 Aharonian, F. A., et al., 2009, *A&A*, 502, 749
 Albert, J., et al., 2007a, *ApJ*, 669, 862
 Albert, J., et al., 2007b, *ApJ*, 66, L17
 Albert, J., et al., 2008, *Science*, 320, 1752
 Anderhub, H., et al., 209, *ApJ*, 704, L129
 Begelman, M. C., Fabian, A. C., & Rees, M. J., 2008, *MNRAS*, 384, L19
 Blandford, R. D., & Levinson, A., 1995, *ApJ*, 441, 79
 Blażewski, M., et al., 2000, *ApJ*, 545, 107
 Bloom, S. D., & Marscher, A. P., 1996, 461, 657
 Böttcher, M., & Chiang, J., 2002, *ApJ*, 581, 127
 Böttcher, M., & Dermer, C. D., 2002, *ApJ*, 564, 86
 Böttcher, M., et al., 2007, *ApJ*, 670, 968
 Böttcher, M., Reimer, A., & Marscher, A. P., 2009, *ApJ*, 703, 1168
 Böttcher, M., & Dermer, C. D., 2010, *ApJ*, 711, 445
 Böttcher, M., & Principe, D., 2009, *ApJ*, 692, 1374
 Bramel, D. A., et al., 2005, *ApJ*, 629, 108
 Collmar, W., et al., 2010, *A&A*, submitted
 Dermer, C. D., Schlickeiser, R., & Mastichiadis, A., 1992, *A&A*, 256, L27
 Dermer, C. D., & Schlickeiser, R., 1993, *ApJ*, 416, 458
 Dermer, C. D., Sturmer, S. J., & Schlickeiser, R., 1997, *ApJS*, 109, 103
 Dwek, E., & Krennrich, F., 2005, *ApJ*, 618, 657
 Edelson, R. A., & Krolik, J. H., 1988, *ApJ*, 333, 646
 Finke, J. D., et al., 2007, *A&A*, 447, 513
 Finke, J. D., Razzaque, S., & Dermer, C. D., 2010, *ApJ*, 712, 238
 Fossati, G., et al., 1998, *MNRAS*, 299, 433
 Fossati, G., et al., 2000, *ApJ*, 541, 166
 Franceschini, A., Rodighiero, G., & Vaccari, M., 2008, *A&A*, 487, 837
 Georganopoulos, M., & Marscher, A. P., 1998, *ApJ*, 506, 621
 Georganopoulos, M., & Kazanas, D., 2003, *ApJ*, 594, L27
 Georganopoulos, M., Finke, J. D., & Reyes, L. C., 2010, *ApJ*, 714, L157
 Giannios, D., Uzdensky, D. A., & Begelman, M. C., 2009, *MNRAS*, 395, L29
 Ghisellini, G., & Madau, P. 1996, *MNRAS*, 280, 67
 Ghisellini, G., et al., 1998, *MNRAS*, 301, 451
 Ghisellini, G., Tavecchio, F., & Chiaberge, M., 2005, *A&A*, 432, 401
 Ghisellini, G., & Tavecchio, F., 2008, *MNRAS*, 386, L28
 Ghisellini, G., & Tavecchio, F., 2009, *MNRAS*, 397, 985
 Gilmore, R. C., et al., 2009, *MNRAS*, 399, 1694
 Graff, P. B., Georganopoulos, M., Perlman, E. S., & Kazanas, D., 2008, 689, 68
 Hartman, R. C., et al., 2001, *ApJ*, 558, 583
 Horan, D., et al., 2009, *ApJ*, 695, 596
 Joshi, M., 2009, Ph.D. Thesis, Ohio University
 Kataoka, J., et al., 2000, *ApJ*, 528, 243
 Kelner, S. R., & Aharonian, F. A., 2008, *Phys. Rev. D.*, 78, 034013
 Kirk, J. G., et al., 2000, *ApJ*, 542, 235
 Kusunose, M., Takahara, F., & Li, H., 2000, *ApJ*, 536, 299
 Li, H., & Kusunose, M., 2000, *ApJ*, 536, 729
 Mannheim, K., & Biermann, P. L., 1992, *A&A*, 253, L21
 Mannheim, K., 1993, *A&A*, 221, 211
 Maraschi, L., Celotti, A., & Ghisellini, G., 1992, *ApJ*, 397, L5
 Marscher, A. P., & Gear, W. K., 1985, *ApJ*, 298, 114
 Mastichiadis, A., & Kirk, J. G., 1997, *A&A*, 320, 19
 Mimica, P., Aloy, M. A., Müller, E., & Brinkmann, W., 2004, *A&A*, 418, 947
 Mücke, A., et al., 2000, *Comp. Phys. Comm.*, 124, 290
 Mücke, A., & Protheroe, R. J., 2000, *AIP Conf. Proc.*, 515, 149
 Mücke, A., & Protheroe, R. J., 2001, *Astropart. Phys.*, 15, 121
 Mücke, A., et al., 2003, *Astropart. Phys.*, 18, 593
 Mukherjee, R., et al., 1997, *ApJ*, 490, 116
 Mukherjee, R., et al., 1999, *ApJ*, 527, 132
 Prandini, E., et al., 2010, *MNRAS*, in press (arXiv:1003.1674)
 Rachen, J., & Mészáros, P., 1998, *Phys. Rev. D*, 58, 123005
 Sbarufatti, B., Treves, A., & Falomo, R., 2005, *ApJ*, 635, 173
 Schlickeiser, R., 1996, *A&AS*, 120, 481
 Sikora, M., Begelman, M., & Rees, M. 1994, *ApJ*, 421, 153
 Sikora, M., et al., 2001, *ApJ*, 554, 1
 Sokolov, A., Marscher, A. P., & McHardy, I. A., 2004, *ApJ*, 613, 725
 Sokolov, A., & Marscher, A. P., 2005, *ApJ*, 629, 52
 Spada, M., Ghisellini, G., Lazzati, D., & Celotti, A., 2001, *MNRAS*, 325, 1559
 Stecker, F. W., Malkan, M. A., & Scully, S. T., 2006, *ApJ*, 648, 774
 Takahashi, T., et al., 1996, *ApJ*, 470, L89
 Tavecchio, F., & Ghisellini, G., 2008, *MNRAS*, 385, L98
 Villata, M., & Raiteri, C. M., 1999, *A&A*, 347, 30
 von Montigny, C., et al., 1995, *ApJ*, 440, 525
 Wagner, S., & Behera, B., 2010, 10th HEAD Meeting, Hawaii (BAAS, 42, 2, 07.05)
 Weidinger, M., Rüger, M., & Spanier, F., 2010, *Astrophys. & Space Sciences Transactions*, vol. 6, Issue 1, p. 1 (arXiv:1001.2145)
 Zhang, Y. H., et al., 2002, *ApJ*, 572, 762



MAX-PLANCK-GESELLSCHAFT



RadioNe